Biogenic volatile organic compounds (BVOCs) reactivity related to new particle formation (NPF) over the Landes forest

J. Kammer, P.-M. Flaud, A. Chazeaubeny, Raluca Ciuraru, K. Le Ménach, E. Geneste, H. Budzinski, J.M. Bonnefond, Eric Lamaud, E. Perraudin, et al.

Title: Biogenic Volatile Organic Compounds (BVOCs) reactivity related to New Particle Formation (NPF) over the Landes forest

Authors: J. Kammer[a,b,c,d,#], P.-M. Flaud[a,b], A. Chazeaubeny[a,b], R. Ciuraru[a,b,##], K. Le Menach[a,b], E. Geneste[a,b], H. Budzinski[a,b], J.M. Bonnefond[c,d], E. Lamaud[c,d], E. Perraudin[a,b] and E. Villenave[a,b,*]

Affiliations and addresses:

[a] University of Bordeaux, EPOC, UMR 5805 CNRS, 33405 Talence Cedex, France

[b] CNRS, EPOC, UMR 5805 CNRS, 33405 Talence Cedex, France

[c] INRA, UMR 1391 ISPA, F-33140 Villenave d'Ornon, France

[d] Bordeaux Sciences Agro, UMR 1391 ISPA, F-33170 Gradignan, France

Now at: School of Chemistry and Environmental Research Institute, University College Cork, Cork, Ireland

Now at: UMR 1402 ECOSYS, INRA-AgroParisTech, Université Paris-Saclay, Thiverval-Grignon, 78850, France

[*]**Corresponding author**:

Eric Villenave

UMR CNRS 5805 EPOC – OASU - University of Bordeaux –

Bâtiment B18N, Allée Geoffroy Saint-Hilaire

CS 50023, 33615 PESSAC CEDEX, FRANCE

Mail: eric.villenave@u-bordeaux.fr

Tel: +33 5 4000 6350

Abstract

Atmospheric particles play a major role in both air quality and climate change. Formation of secondary particles in the atmosphere has been observed over many different environments and is believed to provide up to half of the atmospheric cloud condensation nuclei (CCN) at a global scale. However, high uncertainties are still remaining in the description of mechanisms involved in new particle formation (NPF). Especially, more evidences of the implication of biogenic volatile organic compounds (BVOCs) in NPF from field studies are still needed. To investigate this question, two field campaigns have been set up during July 2014 and July 2015, in the French Landes forest (south west of France). Summer 2015 was characterised by a strong hydric stress, whereas summer 2014 was rainy. In 2015, frequent nocturnal NPF was observed, reaching a frequency of occurrence of ~55% of the nights, while only one event was observed in 2014. In July 2015, monoterpene mixing ratios (dominated by α- and β-pinene) were higher, mostly due to high ambient temperatures and drought. A focus was made on the 2015 field campaign, where NPF was mostly observed. The mean diurnal variation of the ratio between α- and β-pinene mixing ratios highlighted in-canopy reactivity of monoterpenes with ozone in the early night. This hypothesis was reinforced by the increasing gas phase levels of pinonaldehyde and nopinone, the main first-generation products arising from α- and β-pinene ozonolysis, at night, before NPF started. It strongly suggests that monoterpene oxidation further generated very-low volatility gases involved in NPF. This finding is also supported by the high concentrations of the SOA traditional biogenic tracers, *e.g.* pinic and pinonic acids, quantified in the particulate phase. The role of BVOCs in NPF is thus highlighted, as well as the importance of nighttime NPF.

Keywords: Monoterpenes, BVOCs, oxidation products, nighttime NPF, Landes forest

Highlights

- High monoterpene mixing ratios were related to high nighttime NPF frequency.
- In canopy α- and β-pinene ozonolysis was highlighted in the evening.
- Nopinone and pinonaldehyde levels increase before NPF started.
- Biogenic tracer (pinic and pinonic acids) concentration levels were high in the particulate phase.
- BVOC oxidation was strongly involved in nighttime NPF in the Landes forest.

1 Introduction

Forest ecosystems are key components of our environment, representing around 30% of the Earth land surface (United Nations food and agricultural organization, 2015). Also, forests represent a large source of Volatile Organic Compounds (VOCs). It is widely recognized that 90% of VOCs are emitted by biogenic sources, isoprene and monoterpenes being the most emitted biogenic VOCs (BVOCs) in the atmosphere (Guenther et al., 1995; Sindelarova et al., 2014). Once oxidized in the atmosphere, some of their products have sufficiently low volatility to partition between the gas and the particle phases. Through this process, forests act as a source of secondary organic aerosol (SOA), which play a crucial role in air quality and climate change (Hallquist et al., 2009; IPCC, 2013; Kazil et al., 2010; Pope III and Dockery, 2006).

New Particle Formation (NPF) is a process that consists of the secondary formation of atmospheric particles (Dal Maso et al., 2005). Currently, NPF is estimated to contribute around half of the global Cloud Condensation Nuclei (CCN) at a global scale (Merikanto et al., 2009). NPF was observed in a large number of locations worldwide (Kulmala et al., 2004). However, processes governing NPF remain quite uncertain (Andreae, 2013; Kulmala et al., 2013; Nallathamby et al., 2014). Until recently, it was accepted that NPF could not occur without the involvement of sulphuric acid in the first step, *i.e.* nucleation (Andreae, 2013; Kulmala, 2003; Kulmala et al., 2013; Nallathamby et al., 2014). In the atmosphere, gas phase sulphuric acid is mainly generated from SO_2 reaction with OH radicals in the presence of water. It may also be produced in the gas phase by oxidation of SO_2 with H_2O_2 or by reaction with Criegee intermediates (Sipilä et al., 2014). Due to its very low vapour pressure, sulphuric acid may easily form clusters with other molecules, *i.e.* water or oxygenated molecules (Elm et al., 2014; Kulmala, 2003; Neitola et al., 2015; Praplan et al., 2015; Riccobono et al., 2014). Then, if this cluster is stable, it can grow through the condensation of extremely low volatility organic compounds (ELVOCs), produced from autoxidation (Ehn et al., 2014; Kulmala et al., 2013; Praplan et al., 2015; Riccobono et al., 2014). Recently, it was

demonstrated from laboratory studies that NPF can be caused solely by α-pinene ozonolysis (Kirkby et al., 2016; Tröstl et al., 2016). It was highlighted from the CLOUD chamber experiments that highly oxidized molecules (like HOMs) can be rapidly formed, and induce NPF, following autoxidation mechanisms (Ehn et al., 2014; Jokinen et al., 2014). Direct evidence of such implication of HOMs in the real atmosphere was highlighted very recently in the free troposphere, where one of the main driver of NPF could be anthropogenic VOCs (Bianchi et al., 2016). More, Rose *et al*. (2018) observed that biogenic ions can induce stable cluster formation. But identification of biogenic NPF still needs more investigations in real atmosphere, especially at pristine locations. As a consequence, new measurements in ecosystems poorly or not yet investigated are needed.

In this context, the goal of the present study was to reinforce our knowledge on the relation between BVOCs and NPF. For that purpose, two field measurement campaigns took place in the summers of 2014 and 2015 in the Landes forest, in the south west of France. A first paper by our group recently evidenced frequent nocturnal NPF in 2015, together with high monoterpene mixing ratios (Kammer et al., 2018). This new paper first presents a comparison between 2014 and 2015 field campaigns. Then, the focus is made on the main emitted BVOCs at the measurement site, their reactivity and their oxidation products both in the gas and the particulate phases. Finally, considering the recent findings, the link between in canopy BVOC reactivity and NPF is discussed.

2 Methodology

2.1 Site description

As part of the LANDEX-episode zero project, two intensive field campaigns were conducted, in the French Landes forest. The first campaign started from the 5th of July until the 18th of July 2014, and the second started from the 5th to the 23rd of July 2015. The measurement site, located at Bilos (44°29'39.69"N, 0°57'21.75"W, and 37 m above sea level) in the northern part of the Landes forest, is a measurement site of the European Integrated Carbon

Observation System (ICOS). The nearest urban area is Bordeaux and surroundings, at 40 km northeast, and the Atlantic Ocean is 23 km west of the site. The measurement area is a maritime pine (*Pinus pinaster* Aiton) stand sowed in 2004, with an understorey mostly composed of gorse (*Ulex europaeus* L.), grass (*Molinia caerula* (L.) Moench) and heather (C*alluna vulgaris* (L.) Hull). Tree height was around 7 m in 2014 and 8 m in 2015, over a sandy hydromorphic podzol. A more complete description of Bilos site can be found elsewhere (Moreaux *et al*., 2011; Kammer et al., 2018). Due to the proximity of the Atlantic Ocean, the local climate is oceanic, and winds are consequently frequently originating from west-north west.

2.2 Field measurements

Meteorological parameter measurements have been performed on a mast during each campaign, at 15 m above ground level (a.g.l.). Air temperature and relative humidity (HMP 155, VAISALA HUMICAP), wind speed and direction (Windsonic 1, Campbell scientific), global solar radiation (CMP22 and CNR4, Campbell scientific) and rainfall was continuously measured at a half hourly scale. To complete these meteorological measurements, air mass backward trajectories have been computed using the NOAA HYSPLIT model (Stein et al., 2015). Daily backward trajectories were calculated for each day of the campaign using the GDAS (Global Data Assimilation System) meteorological dataset, indicating the origin of the analysed air mass at Bilos. Besides, eddy covariance fluxes of momentum, heat, water vapour and CO_2 were measured at 15 m a.g.l., in order to evaluate the physiological state of the ecosystem. The details of the eddy covariance methods have been fully described elsewhere (Aubinet et al., 2000; Burba and Anderson, 2010).

A mobile laboratory truck (the “Barracuda” facility), located in the centre of the area, was used for physico-chemical measurements with air tubing devoted to aerosol and gas sampling being located at 4 m a.g.l., corresponding to the canopy level. A 5 m Teflon tubing (4.5 mm inner diameter) was used for the gas phase measurements, whereas a 4 m long

conductive silicone tubing (4.5 mm inner diameter) was used to sample particles. Both gas and particle sampling inlets were located right next (about 20 cm) to ensure the collection of the same air masses. Preliminary tests were performed by measuring the same air with and without tubing. As no difference was observed, it is assumed that no significant wall losses of terpenes occurred in tubing. During the campaign, ozone and nitrogen oxides (NO_x = NO + NO_2) mixing ratios were monitored through a UV absorption analyzer (APOA 370, HORIBA, detection limit (DL) = 0.5 ppb) and a chemiluminescence analyzer (APNA 370, HORIBA, DL = 0.5 ppb), respectively. Sulphur dioxide (SO_2) measurements were performed only during the 2015 field campaign using a UV fluorescence monitor (API 100 E, Teledyne, DL = 0.4 ppb). All the three monitors (O_3, NO_x and SO_2) have been calibrated before the campaigns, and leak checks were frequently performed using activated charcoal air filters. A scanning mobility particle sizer (SMPS, TSI model 3080) was used to characterize particle number size distribution every 10 minutes. It combines a differential mobility analyser (DMA, TSI model 3081) and an optical counter (CPC, TSI model 3772). Aerosol flow and sheath flow were set respectively to 0.5 L min^{-1} and 5 L min^{-1} to ensure a 1:10 ratio in the DMA. Under these flow conditions, particle number size distribution and concentration were measured for particles having an electric mobility diameter between 10.9 nm and 487 nm. Particle wall losses were calculated following the methodology described in Baron and Willeke (2001). The estimated particle loss rates were estimated to be 34.7% for the smallest particles (with a 10.9 nm diameter) analysed. The particle number and size distribution data were corrected to account for the calculated wall losses. Then, a proton transfer reaction - time of flight - mass spectrometry (PTR-TOF-MS, Kore Technology) was used to study the composition of the gaseous phase, especially the evolution of BVOCs and their related oxidation products. This instrument is based on the proton transfer reaction from H_3O^+ to the analytes, a soft ionisation which prevents from strong fragmentation. Basically, the air mass composition could thus be analyzed by recording the temporal evolution of the MH^+ ions. During the campaign, the PTR-TOF-MS was operated at 600 V drift voltage and 1.3 mbar reactor pressure, ensuring an E/N ratio around 130 Td (1 Townsend = 10^{-17} V cm^{-2}), with E being the

electric field strength in the reactor and N the gas number density. The PTR-TOF-MS was tuned to work at this E/N ratio as it is a good compromise to prevent from high fragmentation in the mass spectrometer and ambient relative humidity effect (Pang, 2015; Tani et al., 2003). PTR-TOF-MS blanks and calibrations were daily performed using the vapour pressure (at 0°C and diluted in N_2 flow) of a pure α-pinene solution, regulated by a mass flow controller (Millipore, Coastal Instruments). Typical day to day sensitivity variations were about 10 %. The variation of the sensitivity may be sometimes larger, when the PTR-TOF-MS parameters (for example, the voltage applied to extraction lenses) were optimized during the campaign. For non-calibrated compounds (other than α-pinene), calibration coefficients determined for α-pinene were used to consider the day-to-day sensitivity variations of the instrument. But as we could not consider that these calibration coefficients provide a real estimation of the concentration of these other compounds, then each signal was normalized by its maximum count number.

As monoterpenes $C_{10}H_{16}$ present many isomers and as the PTR-TOF-MS was only able to measure their total concentrations, an online gas chromatograph coupled to a flame ionization detector (GC-FID, airmoVOC, Chromatotec) was used to discriminate their speciation. The GC-FID sampled air at 0.11 L min^{-1}, and concentrated VOCs on a cold air trap composed of adsorbent Tenax TA (20–35 mesh, Chrompack). The desorbed VOCs to analyse were then separated using a Chrompack Sil 8CB low bleed capillary column, and finally detected with the FID. A complete description of the GC-FID can be found elsewhere (Staudt and Lhoutellier, 2011). In 2015, the GC-FID was only available during the last five days of the campaign.

The chemical composition of particles collected during the 2015 field campaign was investigated using high performance liquid chromatography coupled to mass spectrometry. Briefly, a high volume sampler (DA-80, Digitel, with an air flow set to 30 m^3 h^{-1}) was used to collect $PM_{2.5}$ (particles with an aerodynamical diameter smaller than 2.5 µm) onto quartz fiber filters (Ø = 150 mm). Different laboratory tests showed that ultrasonic extraction provides the

highest and more reproducible extraction yields. If there are still some uncertainties related to this technique, it is widely used to measure pinic acid and pinonic acid in aerosol samples (Anttila et al., 2005; Feltracco et al., 2018; Kourtchev et al., 2014; Nozière et al., 2015). As a result, particles were extracted two times by placing a 47 mm diameter disc in 3 mL of a mixed acetonitrile/water solution (70/30) under ultrasonication for 15 min. Then, each extract was centrifugated and the supernatent was transfered in a 15 mL vial and concentrated to about 400 µL under a gentle pure nitrogen flow (99.995 % purity, Linde Gas SA) at 40 °C. Samples were weighted using gravimetry (precision: 10^{-4} g), then stored at -18°C until analysis. LC-HRMS analyses were carried out using an Agilent 1290 HPLC system coupled to an Agilent 6540 QToF mass spectrometer equipped with an Agilent Jet Stream electrospray ionization source (ESI) operating in the negative mode. The chromatographic separation was performed on a Zorbax Eclipse XDB-C18 (2.1×150 mm; 3.5 µm) regulated at 30°C. Gradient LC elution was performed at a flow rate of 0.5 mL min^{-1} using 0.2% formic acid in purified water as mobile phase A and 0.2% formic acid in acetonitrile as mobile phase B. Sample injection volume was set at 5 µL. In this study, pinic acid and pinonic acid were quantified using authentic standards of the two targeted compounds (pinic acid 98 % and cis-pinonic acid 98 %, Sigma-Aldrich) as external standards. More details about LC-QTOF-MS parameters can be found in the supplementary information (**Table S1**).

3 Results and discussion

3.1 Meteorological conditions during 2014 and 2015 field campaigns

Meteorological parameters are crucial as they may greatly influence BVOC emissions and the oxidative capacity of the atmosphere. The Bilos site is for instance frequently subject to periods of large hydric stress during summer. Detailed meteorological conditions during 2014 and 2015 field campaigns can be found in **Figures S1** and **S2**. For each campaign, the conditions were very different. The 2015 field campaign was very hot, with few rain events (see **Figures S1.a, d** and **Figures S2.a, d)**. During this last campaign, the air temperature

frequently exceeded 30°C during the day and was hardly ever below 15°C at night, which was not the case in July 2014. Such high temperature values were already reported to induce a thermic stress on trees (Laothawornkitkul et al., 2009). One particularity of the site was that relative humidity increased to reach its maxima (*i.e.* 100%) almost every night, in both July 2014 and 2015.

No rainfall was observed from the middle of June 2015 (meteorological parameters outside the campaign range are available from the ICOS network) and only few mm of rain was recorded between the 5th and the 22nd July in 2015. As a result, a very weak water vapour flux was observed in July 2015, whereas the sensible heat flux was very high (**Figure S2.b**), especially comparing to 2014 fluxes (**Figure S1.b**). The Bowen ratio (between sensible heat fluxes and water vapour fluxes) is a powerful tool to evaluate the hydric stress level. During drought, the water vapour fluxes decrease whereas the heat fluxes increase (by compensation to conserve the energy balance), making the Bowen ratio particularly elevated. Indeed, the 2015 campaign was characterized by Bowen ratio values about 10, which is very high for a forest stand (Gu et al., 2006). Such high Bowen ratios were not observed during the 2014 field campaign, with values only around 0.5 (Kammer et al., 2019). Thus, a thermic stress (due to temperatures over 30°C) coupled to a hydric stress occurred during the 2015 campaign. The presence of such a stress situation may increase BVOC emissions (Kesselmeier and Staudt, 1999; Laothawornkitkul et al., 2009; Loreto et al., 1998; Peñuelas and Staudt, 2010). Wind directions indicated that air masses were mostly coming from west-northwest direction in 2014 as well as in 2015 (**Figures S1.e** and **S2.e**), which was confirmed by backward air mass trajectories calculations. Air masses were thus mostly influenced by the Atlantic Ocean in both campaigns.

3.2 General conditions of the campaigns

A previous study reported by our group (Kammer et al., 2018) showed that NPF has been frequently observed during the 2015 field campaign, mostly during the night, although a few

events (only 2) were also recorded during daytime. NPF events were defined as an increase of particle concentration in the nucleation mode followed by a subsequent growth during at least 2 hours (Dal Maso et al., 2005). In 2014, only one NPF event was observed, occurring during nighttime. This leads to a NPF frequency of occurrence (i.e. the number of nights where NPF events were observed divided by the total number of nights during the field campaign) of about 8% during the 2014 field campaign. In 2015, 12 NPF events were reported, reaching a high frequency of occurrence of around 55% (Kammer et al., 2018). NPF thus occurred more frequently in a summer influenced by a hydric stress (according to the high Bowen ratio values measured during the 2015 campaign). This observation may further suggest that the presence of a hydric stress is indirectly inducing more NPF events because of stronger monoterpene emissions. Nevertheless, more studies about the effect of hydric stress on NPF will be needed to confirm such hypothesis. All the observed NPF events are listed in **Table S2**. A more complete analysis of NPF events (growth rates, nucleation rates, etc.) can be found in Kammer et al. (2018).

Analyses of wind directions and air mass back trajectories have shown that air mass origin did not affect NPF. During both campaigns, NPF were always recorded along (i) high relative humidity (i.e. RH ≥ 75%), (ii) temperatures higher than 16°C and (iii) 1/u* (where u* is the friction velocity) over 2.5 s m^{-1}, indicating vertical stratification (this parameter was usually below 2 s m^{-1} during the day where turbulence occurred, see the meteorological parameters in **Figures S1** and **S2** during NPF events). It shows that NPF started once the stable nocturnal boundary layer was taking hold. As suggested by the air mass analysis, nocturnal NPF were very likely influenced by local emissions, limiting the impact of transported compounds.

NO, NO_2, SO_2 (only for 2015 campaign) and ozone mixing ratios are represented on **Figures S3** and **S4**. NO_x mixing ratios were very low during both campaigns, confirming the very rural feature of the Bilos site. The mixing ratios of SO_2, which is recognized as a key species for daytime nucleation, was always around the DL value of the instrument (only available in

2015, **Figure S4.b**). As a consequence, and taking into account the nocturnal nature of NPF, it is highly probable that sulphuric acid was not responsible for nocturnal NPF at Bilos, conversely to classical daytime NPF. Ozone mixing ratios presented a typical diurnal cycle with maximal values reached during the afternoon, and frequently dropped under the analyser limit (*i.e.* 0.5 ppb) in the middle of the night. The nights of July 15th and 16th in 2014 and 12th to 15th, 17th, 18th and 20th in 2015 are perfect examples of this ozone drop (**Figures S3.c** and **S4.c**). The meteorological conditions observed during these nights indicate that these ozone drops occurred under stratified atmosphere conditions (low wind speed and high 1/u*).

3.3 Monoterpene mixing ratios

The sum of monoterpene as well as ozone mixing ratios are represented in Figure 1 for both field campaigns. A strong diurnal cycle was observed in July 2014 as well as in July 2015 for both ozone and monoterpenes. A typical ozone diurnal cycle was observed, with higher values in the afternoon (Figure 1). The ozone cycle was mirrored by the monoterpenes cycle, with higher monoterpene mixing ratios values during the night, as previously reported in the Landes forest (Simon et al., 1994). Monoterpenes were dominated from far by α- and β-pinene, accounting for around 90% of total monoterpenes, in accordance with previous studies (Riba et al., 1987; Simon et al., 1994). Maritime pines are well-known to be strong temperature driven BVOC emitters (Kesselmeier and Staudt, 1999; Lathiere et al., 2006). Although emissions are higher during the day, the larger dilution of emissions in the surface layer and the higher oxidant levels conduct to lower BVOC mixing ratios during light hours. More explanation about the diurnal cycle and the effect of the change in the boundary layer height on monoterpene mixing ratios can be found in Kammer *et al*. (2018). In 2015, monoterpene mixing ratios frequently (*i.e.* almost half of the nights) reached around 15 ppb, whereas they were always lower than 10 ppb in 2014, except the night of July 16th to 17th (**Figure 1**). The highest values were reached the 21st of July 2015, where the sum of monoterpene mixing ratios exceeded 35 ppb (**Figure 1.b**). The very high mixing ratios of

296 monoterpenes observed in 2015 were assumed to be the result of the meteorological
297 conditions, and more specifically the thermic/hydric stress. The high frequency of occurrence
298 of NPF in 2015 occurred for the highest monoterpene mixing ratios, emphasizing the role of
299 monoterpenes at night at Bilos.

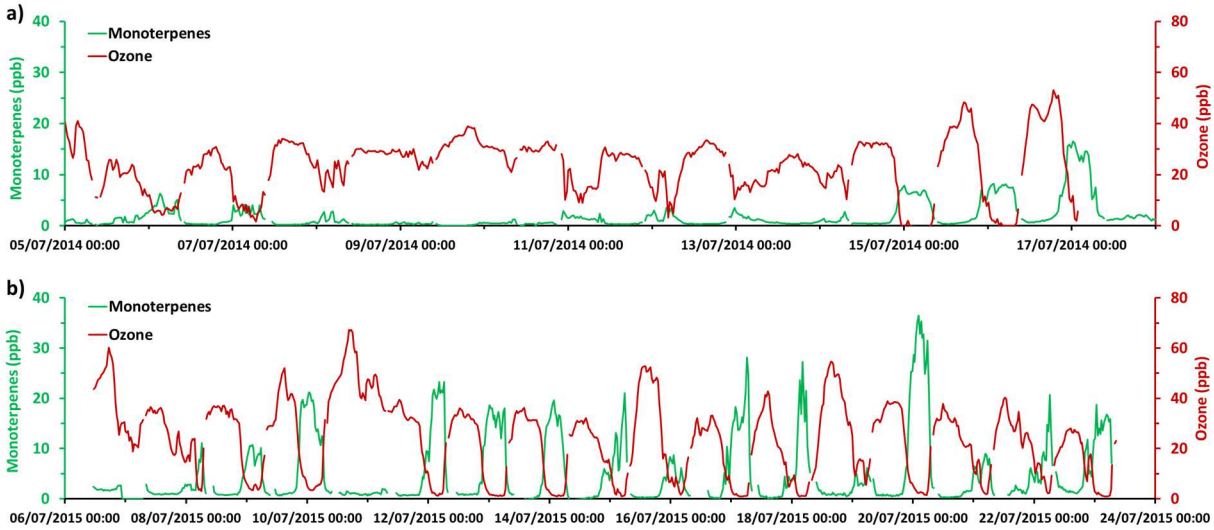

Figure 1: Time series of the sum of monoterpene mixing ratios (in ppb, green line) and ozone mixing ratios (in ppb, red line) for **a)** 2014 and **b)** 2015 field campaigns.

300 ### 3.4 Monoterpene/O_3 reactivity

301 Time series of ozone and monoterpene mixing ratios (**Figure 1**) suggest that their respective
302 diurnal cycles were closely anti-correlated. The monoterpene mixing ratios increased every
303 night, as reported on **Figure 1**, when it is likely that no ozone was produced (because of its
304 dependence on solar radiation), nor ozone advection from higher layers of the atmosphere
305 (because of the nocturnal stratified boundary layer). The anti-correlation between ozone and
306 monoterpenes can be observed on **Figure 2.a**. Interestingly, when ozone was close to 0,
307 monoterpene mixing ratios values were at least of 5 ppb during the corresponding nights
308 (**Figure 2.a**). Reaction between ozone and monoterpenes in the early night could thus be
309 expected. Such reactions could only partially explain the ozone drop to levels close to zero,
310 as their kinetic rate constants are quite low (Atkinson and Arey, 2003). A rough estimation,
311 assuming pseudo-first order reactions between ozone and monoterpenes, led to a maximal

312 contribution to the ozone decrease being around 50 %. Thus, there is also a possibility for
313 other reactive BVOCs to be co-emitted with monoterpenes and react very fast with ozone
314 (like β-caryophyllene, for example). Further modelling of ozone deposition and chemical
315 reactions between ozone and BVOCs will be needed for a detailed estimation.

316 As monoterpene emissions come from the diffusion of resin stored in pools, the ratio
317 between α- and β-pinene in maritime pine emissions is assumed to be constant (Simon et al.,
318 1994). Hence, changes in the α/β-pinene ratio can mostly be assigned to differences in
319 oxidation processes, as the reactivity of α- and β-pinene with the main atmospheric oxidants
320 differs (see **Table 1**). The daily evolution of the α/β-pinene ratio may provide an interesting
321 tool to evaluate the importance of each oxidation processes. When the OH-initiated
322 monoterpene photooxidation is the dominant process, β-pinene mixing ratio should decrease
323 faster than that of α-pinene, because of its larger reactivity with OH (**Table 1**). In the morning,
324 the α/β-pinene ratio measured at Bilos was increasing, meaning that photooxidation was
325 increasingly dominated by OH radicals (**Figure 2-b**). In the afternoon, the α/β-pinene ratio
326 was found to drop, during both 2014 and 2015 field campaigns. Such decrease reflects that
327 the dominating oxidation process was changing, as the reaction rate constants of α-pinene
328 with ozone and NO_3 are known to be larger than for β-pinene (**Table 1**). It is recognized that
329 NO_3 reactivity is mostly significant during nighttime, as nitrate radicals are photolysed by
330 solar radiations (Seinfeld and Pandis, 2006). As a result, the drop of the α/β-pinene ratio
331 highlighted the dominant role of ozone oxidation processes in the afternoon.

Table 1: Chemical kinetic rate constants of reactions of α- and β-pinene with the main atmospheric oxidants (OH, O_3 and NO_3)

	Rate constant (at 298K, in cm^3 $molecule^{-1}$ s^{-1})		
	OH	O_3	NO_3
α-pinene	$(5.3\pm0.2) \times 10^{-11}$	$(9.0\pm0.2) \times 10^{-17}$	$(6.2\pm0.1) \times 10^{-12}$
β-pinene	$(7.6\pm0.1) \times 10^{-11}$	$(1.9\pm0.3) \times 10^{-17}$	$(2.5\pm0.1) \times 10^{-12}$

IUPAC recommended values (Atkinson et al., 2006)

The **Figure 2.b** shows that the α/β-pinene ratio mean diurnal cycle was more pronounced in 2015. Solar radiation, taken as a simple proxy for OH concentration, and ozone mixing ratios, were higher in 2015 than in 2014 (**Figures 2.c** and **2.d**). Higher OH concentration or ozone mixing ratios led to a more pronounced increase or drop in the α/β-pinene ratio values, respectively. The **Figure 2.b** illustrates that the mean diurnal cycle of the α/β-pinene ratio logically followed the solar radiation and ozone diurnal profiles. The analysis of the mean diurnal evolution of the α/β-pinene ratio also supports the hypothesis of the importance of ozone reactions with monoterpenes in the afternoon/evening. To check this hypothesis, the presence (or absence) of monoterpene oxidation products in the gas phase was investigated.

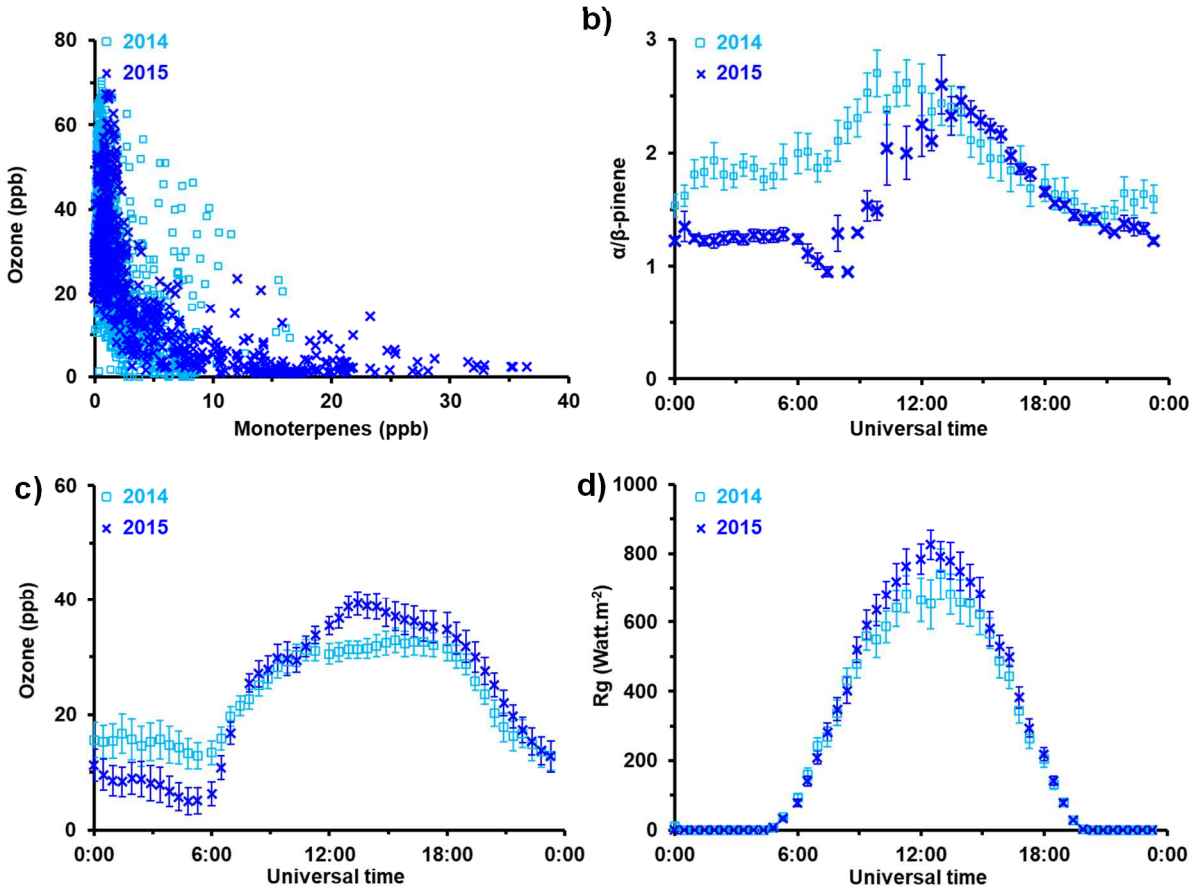

Figure 2: **a)** Anti-correlation between ozone and monoterpene mixing ratios **b)** mean diurnal profile of the α/β-pinene ratio **c)** mean diurnal profile of the ozone mixing ratios **d)** mean diurnal profile of global radiation, during each campaign. The error bars represent the standard errors of each variable. For each graphics, light blue squares represent 2014 dataset, and dark blue crosses represent 2015 dataset. (Universal time = local time – 2h)

343

344 ### 3.5 BVOC oxidation products

345 As the PTR-TOF-MS has a good mass resolution, and considering the high mixing ratios of
346 both α- and β-pinene at the Bilos site, several detected ions were able to be attributed to
347 biogenic oxidation products. The identification of the following ions was proposed based on
348 the proximity of the peak with the theoretical mass, and considering the characteristics of the
349 Bilos site (very rural, high monoterpene mixing ratios, etc.). However, a contribution of a
350 compound with a m/z very closed to the proposed compound could not be fully excluded.

First, m/z 139.11 was proposed to be attributed to nopinone ($C_9H_{14}O$) and m/z 169.12 to pinonaldehyde ($C_{10}H_{16}O_2$), as both compounds were frequently reported at rural field sites (Bourtsoukidis et al., 2014; de Gouw and Warneke, 2007; Park et al., 2014, 2013; Rantala et al., 2014; Ruuskanen et al., 2011). Relevant signals were also observed at m/z 135.11, m/z 151.10 and m/z 155.13, but their attribution was more difficult. The m/z 135.11 protonated ion corresponds to compounds of the molecular formula $C_{10}H_{14}$. Among several potential hydrocarbons, the m/z 135.11 ion may correspond to *p*-cymene, which has already been reported by Gratien *et al*. (2011) as a secondary product of α-pinene photo-oxidation. Even if *p*-cymene has not yet been reported among monoterpene emissions from maritime pines, some works have already pointed out its emission from different plant species (Bäck et al., 2012). *P*-cymene could thus have been be emitted by understorey species (for which BVOC emissions remain unknown or poorly investigated), or result from α-pinene photo-oxidation. *P*-cymene levels were found to be highly correlated with pinonaldehyde and nopinone (R^2 = 0.8), suggesting the secondary origin of this compound.

The molecular formula $[C_{10}H_{14}O]H^+$ was proposed to be the major contributor of m/z 151.10 ion. This ion is recognized as a monoterpene oxidation product, and some studies attributed this mass to a significant pinonaldehyde fragment (de Gouw and Warneke, 2007; Holzinger et al., 2007; Park et al., 2014; Rantala et al., 2014). Note that *i*) other compounds such as myrtenal or verbenone, that may have primary sources, could also be important contributors to the m/z 151.10 signal (Kim et al., 2010) and *ii*) OH initiated oxidation of nopinone was also reported to yield products with m/z 151.10. Finally, the PTR-TOF-MS signal recorded at m/z 155.13 has been identified as $C_{10}H_{18}O$ compounds. Several isomers can potentially contribute to this signal. Notably, primary $OVOC_S$ such as linalool or 1,8-cineol have already been reported at m/z 155.13 elsewhere (Bourtsoukidis et al., 2014; Park et al., 2013; Rantala et al., 2014). However, a contribution of secondary oxygenated compounds cannot be excluded. The presence of all such monoterpene oxidation products confirms that monoterpenes were oxidized at the Bilos site. Especially, pinonaldehyde and nopinone are

known to be exclusively formed from the oxidation (by ozone or OH radical) of α- and β-pinene, respectively, supporting the occurrence and the importance of the oxidation of monoterpenes in the Landes forest. Indeed, OH can be formed as a secondary product of the ozonolysis of monoterpenes. Any observed OH reactivity during nighttime would thus be an indication of a primary monoterpene ozonolysis process. It was finally assumed that the increase of nopinone and pinonaldehyde during the night was arising from monoterpene ozonolysis.

The temporal evolution of the compounds of interest measured during the 2015 field campaign is represented on **Figure 3**. In this section, we make the choice to focus on the 2015 data as *i)* oxidation product concentration values were frequently around the DL of the instrument in 2014 and *ii)* there was only one NPF event in 2014. This is consistent with lower monoterpene mixing ratios observed during this first campaign. As oxidation products were not quantified in this study, their corresponding signals were normalized to their maximum to allow the comparison of their temporal evolution profiles and diurnal dynamics. Interestingly, all the oxidation products globally followed the same diurnal cycle, similar to that observed for monoterpenes (**Figure 3**). Their levels started to increase with the sunset, then decreased when the first rays of the sunlight appeared (**Figure 3**). The decrease of the monoterpene oxidation product could be explained by *i*) a higher dilution due to the increase of the surface layer height as soon as the first rays break the stable nocturnal boundary layer and *ii*) potential photolysis, especially in the case of pinonaldehyde and nopinone, as both are carbonyl compounds prone for photolysis. Although oxidation products are quite volatile and thus are not expected to directly contribute significantly to NPF, they highlight a strong reactivity between ozone and monoterpenes, also yielding (at night) to potential very low volatile oxidation products that may contribute to nocturnal NPF at Bilos.

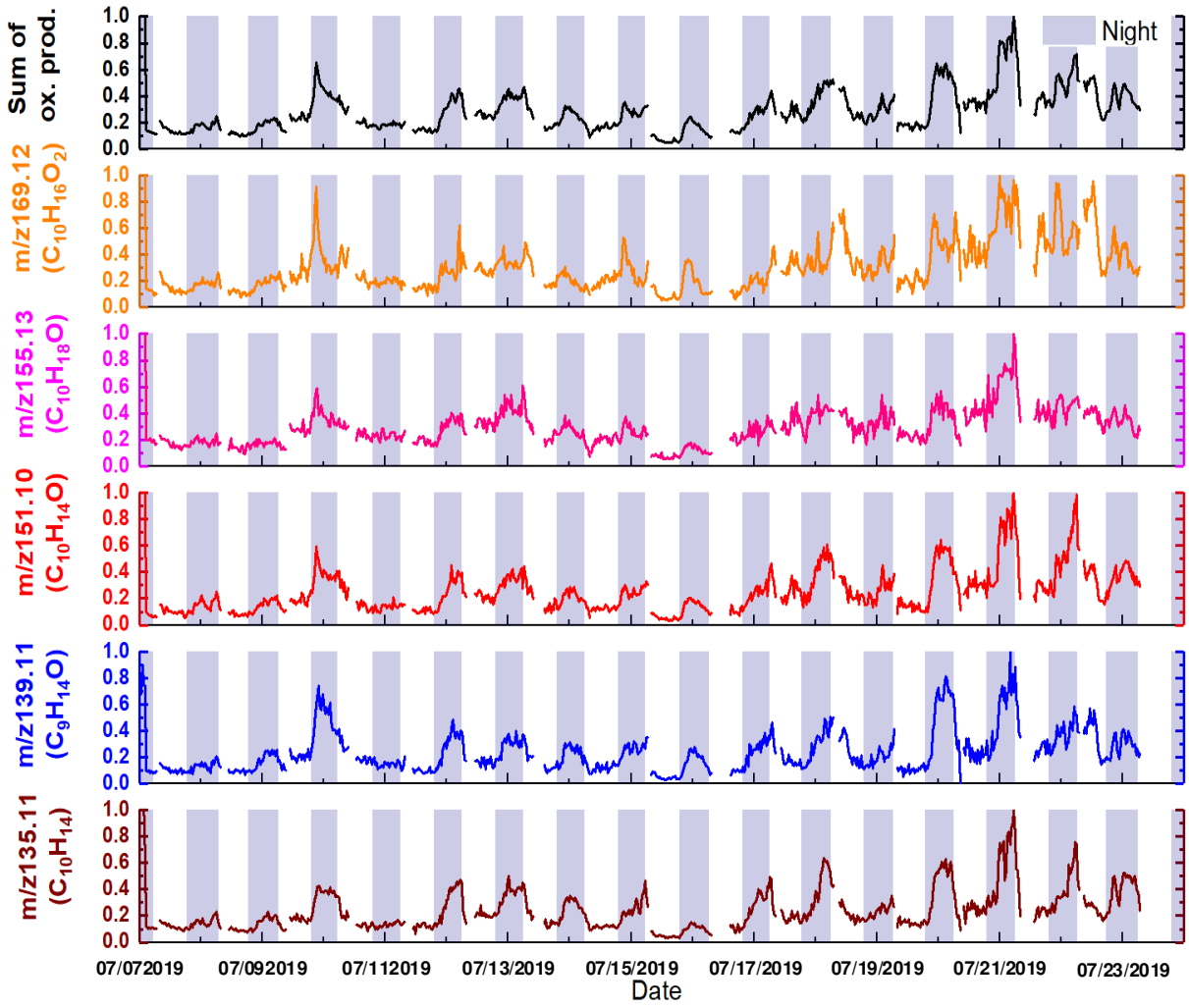

Figure 3: Half hourly evolution of m/z 135.11 ($C_{10}H_{14}$), m/z 139.11 ($C_9H_{14}O$, nopinone), m/z 151.10 ($C_{10}H_{14}O$), m/z 155.13 ($C_{10}H_{18}O$), m/z 169.12 ($C_{10}H_{16}O_2$, pinonaldehyde) and their sum. Y axes are unit less as signals (number of counts) have been normalized to their maximum. Missing data are due to calibrations and blanks of the instrument. The blue shaded areas denote the nighttime periods (defined as the time when global radiation was below 50 W m^{-2}).

3.6 Nighttime reactivity of BVOC oxidation products

In order to go further in the understanding of the role of oxidation products observed in the forest, it was decided to particularly focus on a short period, on m/z 139.11 and m/z 169.12 signals, corresponding to nopinone and pinonaldehyde respectively (**Figure 4**). This is of particular interest as they are directly related to α-pinene (for pinonaldehyde) and β-pinene (for nopinone) oxidation. To the best of our knowledge, no direct comparison of diurnal

409 behaviours of both nopinone and pinonaldehyde from online field measurements has ever
410 been reported. The **Figure 4** presents the temporal evolution of nopinone, pinonaldehyde,
411 total monoterpenes and ozone mixing ratios during two nights (12/13 and 13/14 July 2015),
412 representative of the entire campaign. It can be observed that during both nights,
413 pinonaldehyde signal first increased faster than that of nopinone, reaching its maximum
414 within a few hours and then decreased throughout the night. At the end of the night, a new
415 increase was observed for pinonaldehyde mixing ratios, which finally returned to its daily
416 level in the morning. The nocturnal dynamics of nopinone was observed to be simpler.
417 Nopinone level started to increase at the sunset and decreased in the morning as turbulence
418 reappeared. Such a strong difference between the nocturnal profiles of these two
419 compounds probably results from their different physico-chemical properties and related
420 reactivity. The formation yields of pinonaldehyde and nopinone from ozonolysis of α- and β-
421 pinene have been reported to be highly dependent on the physico-chemical conditions (Lee
422 et al., 2006). More, the range of formation yields for both compounds are quite similar and
423 very large (**Table 2**). If formation yields did not directly allow elucidating the faster increase of
424 pinonaldehyde, the higher reaction rate constant of α-pinene ozonolysis (compared to β-
425 pinene) may at least partially explain such trend.

Table 2: Formation yields of nopinone and pinonaldehyde from β- and α-pinene ozonolysis, reaction rate constants with the main atmospheric oxidants OH, O_3 and NO_3 and saturation vapour pressures (P_s in Torr).

	Compounds	
	Nopinone	Pinonaldehyde
Formation yields (%)	16-40 [a]	6-53 [a]
k_{OH} (cm^3 $molecule^{-1}$ s^{-1})	$(1.7\pm0.2) \times 10^{-11}$ [b]	$(3.9\pm0.2) \times 10^{-11}$ [c]
k_{O3} (cm^3 $molecule^{-1}$ s^{-1})	$< 5 \times 10^{-21}$ [b]	$< 2 \times 10^{-20}$ [c]
k_{NO3} (cm^3 $molecule^{-1}$ s^{-1})	$(1.1\pm0.3) \times 10^{-15}$ [b]	$(2.0\pm0.3) \times 10^{-14}$ [c]
P_s at 298K (Torr)	0.4	0.038 [d]

[a] Lee *et al*. (2006) and references therein [b] Calogirou *et al*. (1999) [c]recommended IUPAC values (Atkinson et al., 2006) [d] Hallquist *et al*. (2009)

The second difference between the two nighttime product time profiles was the decrease of pinonaldehyde during the night, not (or less) observable in the case of nopinone, highlighting a larger sink for pinonaldehyde than for nopinone (**Figure 4**), assumed to be due to its faster reactions with atmospheric oxidants (**Table 2**). The reaction of pinonaldehyde with ozone is known to be very slow, and may not be responsible of such a decrease. NO_3-initiated reaction might be an important removal process for pinonaldehyde but would have required larger concentrations of nitrate radicals that those expected at the very low NO_x levels measured during the campaign (**Figures S3.a** and **S4.a**). In addition, NO_3 reaction rate constants with α- and β-pinene are at least 100 times faster than nopinone and pinonaldehyde (**Table 1**). As a result, any NO_3 radicals present at Bilos would first react with monoterpenes, not allowing to explain the decrease of pinonaldehyde.

Many studies have reported the secondary formation of OH radicals following the monoterpene ozonolysis, with yields up to 1 (Rickard *et al*., 1999; Aschmann *et al*., 2002; Fick *et al*., 2002; Atkinson and Arey, 2003; Forester and Wells, 2011). Moreover, Faloona *et al*. (2001) reported unexpected high OH concentrations at a deciduous forest site during nighttime. Therefore, it is reasonable to hypothesize that the nighttime pinonaldehyde decrease was due to its reaction with OH (this reaction being 5 times faster than that of nopinone) (**Table 2**). Obviously, future measurement of OH radicals at the Bilos site will be required to deeply answer to this question.

Another hypothesis can be put forward to tentatively explain the different profiles of pinonaldehyde and nopinone: their potential condensation on the particle phase. Indeed, the saturation vapour pressures of the two compounds differ by one order of magnitude, pinonaldehyde being 10 times less volatile than nopinone at ambient temperature (**Table 3**). But Kavouras *et al*. (1999) have shown that both compounds are usually mostly present in the gas phase. As a result, gas/particle partitioning might only weakly impact their concentration in the gas phase. Lastly, heterogeneous reactions (as for example, reactions with amines) could not be excluded from this discussion, and may play an important role in the fate of both products (Duporté et al., 2016), but the investigation of such reactions was beyond the scope of the present study and might be considered in the further measurement campaigns at Bilos.

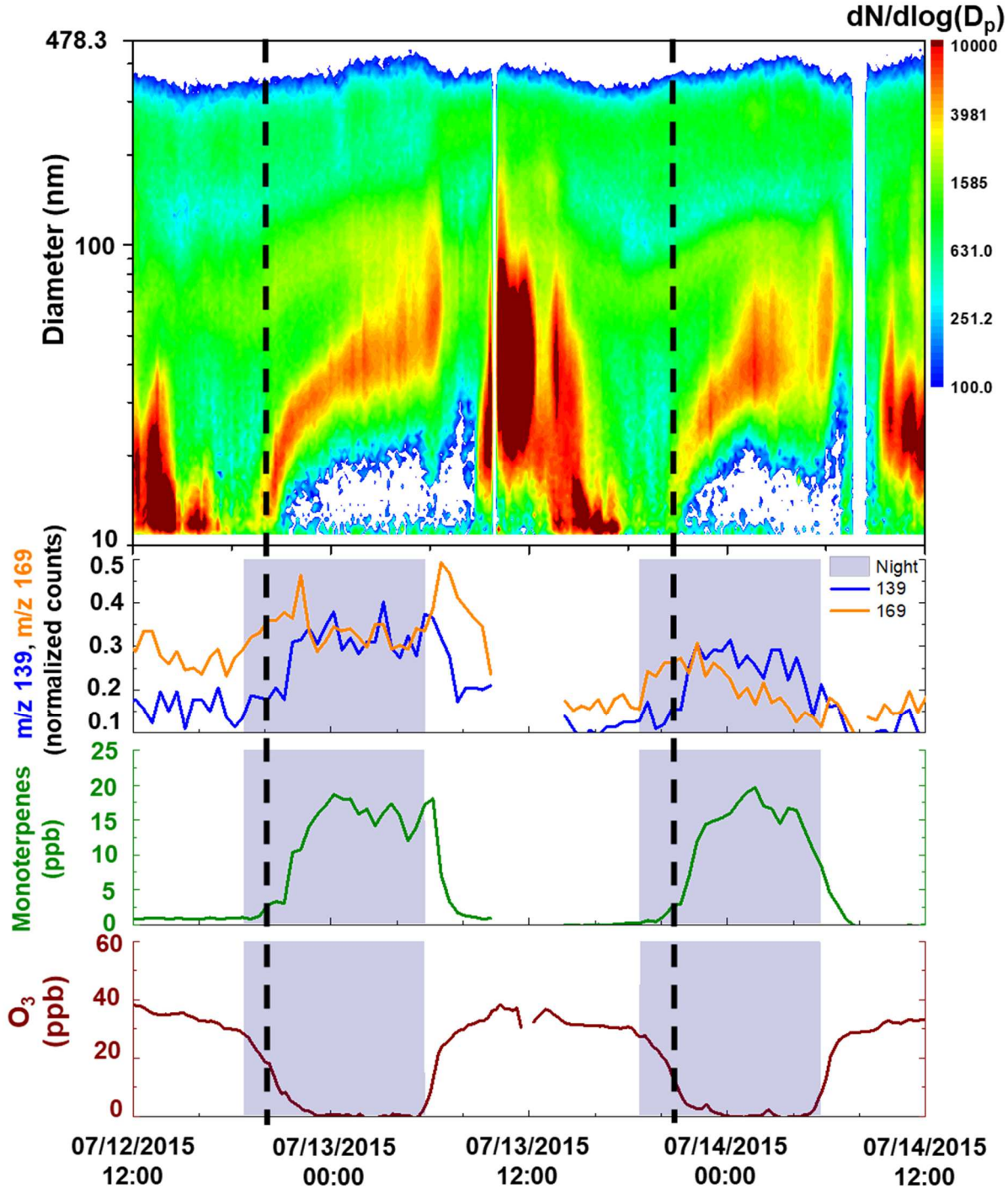

Figure 4: Size distribution of particles between 10 nm and 478.3 nm, during two typical NPF events observed at Bilos in July 2015. On lower panels: the half hourly evolution of m/z 139.21 ($C_9H_{14}O$, nopinone) and m/z 169.24 ($C_{10}H_{16}O_2$, pinonaldehyde) normalized signals, total monoterpene and ozone mixing ratios are represented. Intensities of oxidation product signals (number of counts) have been normalized to their maximum. Blue shaded areas denote the nighttime periods (defined as the time when global radiation was below 50 $W.m^{-2}$).

456

3.7 Contribution of BVOC oxidation products to NPF

This work raises the question of the link between the in-canopy reactivity of monoterpenes and the NPF events observed at night. In a recent paper (Kammer et al., 2018), we reported that NPF always occurred *i*) when the condensation sink was low, *ii*) after the nocturnal boundary layer was taking hold and *iii*) for the nights where monoterpene mixing ratios were high, suggesting their contribution to nocturnal NPF. In the **section 3.5**, we relate that the mixing ratios of monoterpene oxidation products increased at night. The **Figure 4** presents two consecutive nights (12/13 and 13/14 July 2015) where NPF occurred, as a typical example of what was observed during the campaign. At night, the sum of monoterpene mixing ratios started to increase about 1-2 hours before NPF took place, at the same time as nopinone and pinonaldehyde. This time might corresponded to a switch from condensation to nucleation, resulting from the drop of the condensation sink and the higher abundance of low volatile intermediates. To go further, a better knowledge of nanometer particle formation and size-resolved chemical composition of aerosols will be necessary. **Figure 4** shows that monoterpenes and their oxidation products levels increased simultaneously, which means that the main drivers that are triggering NPF are probably physical. However, the time lag between the simultaneous increase and the beginning ot the NPF event may be due to *i*) the inability of the SMPS to catch the first steps of NPF and *ii*) the required time for condensable vapors to reach their saturation limit. This last hypothesis suggests a fast oxidation process, able to generate very low volatile gases in a short time. Auto-oxidation process has been shown to be able to produce highly oxidized multifunctional organic compounds (HOMs) very fast, which can then promote particle nucleation and growth (Jokinen et al., 2014; Kirkby et al., 2016; Tröstl et al., 2016). Hence, simultaneously to nopinone and pinonaldehyde generations, HOMs may have been produced by fast auto-oxidation processes, participating *in fine* to nocturnal NPF (Jokinen et al., 2014). In addition, OH radicals were very probably produced from the ozonolysis of monoterpenes during the night. This is supported by the time evolution of pinonaldehyde, which decreased in the middle of the night, probably due to

its reaction with OH. Thus, secondary reactions involving OVOCs might also be involved in NPF. The lag time described above might also be the time required for these secondary reactions to take place. But, even if the reactions between OH and OVOCs could be important for NPF at Bilos, the main source of OH during nighttime was arising from the primary ozonolysis of monoterpenes, highlighting the importance this process as an initial step. To go further, the contribution of each oxidation pathways (*i.e.* ozone and OH) to NPF will need more investigations. Considering that most of NPF events occurred during nighttime and the very low SO_2 mixing ratios observed at Bilos, it was not expected that sulfuric acid was involved, emphasizing again the role of BVOCs. The recent studies about NPF from pure BVOC ozonolysis, and the high monoterpene mixing ratios at our site let us hypothesise that ozonolysis of monoterpenes - and potentially other BVOCs - may be one of the main drivers of nocturnal NPF at the Bilos site (Kirkby *et al.*, 2016; Tröstl *et al.*, 2016).

3.8 Molecular tracers of BVOC oxidation in the particle phase

To support our hypothesis about the contribution of BVOCs to the nocturnal NPF, SOA tracers from α- and β-pinene oxidation were investigated in the $PM_{2.5}$ particulate fraction collected during the 2015 field campaign. Even if the chemical composition of $PM_{2.5}$ and newly formed particle could be different, it is well-recognized that pinic and pinonic acids are good tracers for SOA formed from α- and β-pinene ozonolysis (Claeys et al., 2009; Faiola et al., 2014; Hallquist et al., 2009; Jaoui et al., 2005; Kristensen et al., 2016; Nozière et al., 2011; Yasmeen et al., 2011). Thus, the presence of such markers in $PM_{2.5}$ would support our hypothsis. During July 2015, pinic and pinonic acids were detected and quantified in all samples. Both products were found in large quantities in the particles collected at Bilos, in every 24 hours filters. Mean concentration of pinic acid was 18.3 ng m^{-3}, and reached the maximum value of 33.8 ng m^{-3} (**Table 3**). These values are in the same order of magnitude as those previously reported in studies conducted in other rural forested areas around the world. For example, the concentration of pinic acid measured in a boreal forest (Hyytiälä, Finland**)** during summertime was 7.2 ng m^{-3}, and reached a maximal concentration of 31 ng

511 m^{-3}. Pinic acid concentrations reported at other sites (**Table 3)** were reported to be beween 4
512 and 8 ng m^{-3}, slightly lower than those measured at Bilos. This is consistent with the high
513 monoterpene mixing ratios presented above. The mean concentrations of pinonic acid during
514 the campaign was 10.2 ng m^{-3}, also close to the reported values in **Table 3**. The high
515 concentrations of these markers arising from α- and β-pinene oxidation measured in this
516 work support the high reactivity between monoterpenes and ozone, which is an important
517 oxidation pathway for monoterpenes during nighttime at the Bilos site. This result attests that
518 oxidation products of pinenes are well transferred to the particle phase, resulting from either
519 gas/particle transfer during NPF or condensation. Further measurements of the size-resolved
520 chemical composition of aerosols will be necessary to differentiate these processes.

521 In the present study, the concentrations of markers in the particle phase were in the same
522 range as the reported values (or around twice as high), whereas monoterpene mixing ratios
523 were at least one order of magnitude higher (**Table 3**). Such differences in the ratio between
524 particulate SOA tracers concentrations and gaseous monoterpene mixing ratios suggest that
525 different physico-chemical processes may occur at our site.

526 To further investigate the link between in-canopy monoterpene reactivity and nocturnal NPF,
527 night and day filter sampling should be performed. Mochizuki *et al*. (2014) observed strong
528 differences in the concentration of night and day particulate SOA tracers. In the case of
529 nocturnal NPF identified in this study, such information could help to unravell the detailed
530 processes. the This will be considered in a next field campaign implemented at Bilos. Note
531 that a large panel of other biogenic SOA tracers were detected in the particles collected. The
532 detailed chemical composition of atmospheric particles collected during the campaign will be
533 the subject of a future publication.

534

535

Table 3: Comparison of pinic and pinonic acid concentrations measured at the Bilos site in

July 2015 and those reported in the litterature

Field site		Pinic acid		Pinonic acid		Monoterpenes	Ref.
Concentrations (ng m^{-3})		Mean	Min – Max	Mean	Min - Max	Mixing ratios (ppb)	
Landes forest (Bilos, France) July 2015		18.3	4.3 – 33.8	10.2	2.2 – 31.7	10 – 30	This work
Boreal forest (Hyytiälä, Finland) July/August 2010/2011		7.2	0.64 – 31	10.7	0.1 - 80	<1	(Vestenius et al., 2014)
Deciduous forest (Jülich, Germany) July 2003		4.2	0.9 – 9.9	-	-	-	(Kourtchev et al., 2014)
Pine plantation (California, USA)							
Sept 2007		7.6	-	6.1	-	0.7 - 2.1	(Kristensen et al., 2013)
July 2009		7.1	-	11	-		
Larch forest (Fujiyoshida, Japan)							
July 2012	Day	4.1	0 – 18.2	12.7	1.7 – 28		(Mochizuki et al., 2014)
	Night	6.4	0.8 – 14.5	3.1	0.9 – 6.8	0.5 - 4.4	

Conclusions

Two intensive field measurement campaigns were conducted in the French Landes forest, at Bilos, in the summers of 2014 and 2015. Frequent nocturnal NPF events were observed during periods of strong thermic and/or hydric stress (dry and hot summer). In parallel, monoterpene mixing ratios (dominated by α- and β-pinene) reached very high levels almost every night, frequently over 20 ppb in summer 2015. A strong anti-correlation between ozone and monoterpene mixing ratios was highlighted, suggesting a high chemical reactivity. This hypothesis was reinforced by the mean diurnal variation of the ratio between α- and β-pinene mixing ratios. Products from the oxidation of α- and β-pinene, namely pinonaldehyde and nopinone, were measured in the gas phase. The diurnal profiles of these two oxidation products is consistent with the high reactivity between α- and β-pinene mostly with ozone in the evening. Furthermore, pinonaldehyde and nopinone presented different nocturnal

548 profiles, suggesting a possible secondary source of OH radicals from monoterpene
549 ozonolysis during the night. Further work will be necessary to adress this issue. The particle
550 phase analysis allowed to identify and quantify pinic and pinonic acids, confirming the
551 oxidation of monoterpenes observed at Bilos as well as the contribution of these precursors
552 to SOA. Considering the differences between 2014 and 2015 field campaigns in the
553 frequency of occurrence of NPF, the monoterpene mixing ratios, and the observed
554 monoterpene in-canopy reactivity, monoterpene ozonolysis is proposed to very likely
555 contribute to nocturnal NPF at our site. Measurements of size-resolved aerosol composition
556 will be required to determine more specifically to which extent monoterpene oxidation
557 products are involved in nucleation and/or aerosol growth in the Landes pine tree forest.

558 The high NPF frequency of occurence observed in 2015 may be associated to the direct
559 consequence of the hydric/thermic stress, which promotes strong BVOC emissions.
560 Considering that the number of hydric stress periods will continue to increase due to the
561 global warming, it can be hypothesized that NPF events may be more and more important in
562 southwestern France. More studies will thus be required to confirm the effect of hydric stress
563 on NPF.

564

565 **Acknowledgements**

566 This work was supported by the French Environment and Energy Management Agency
567 (ADEME), the CNRS-INSU LEFE-CHAT research program, the NEEDS action, and the
568 PEPS IdEx Bordeaux. The authors want to acknowledge the Bilos ICOS team (Christophe
569 Chipeaux, Sébastien Lafont and Denis Loustau) for meteorological data and site availability
570 and Michael Staudt (CEFE-CNRS) for the loan of the GC-FID during the campaign. We also
571 thank Didier Garrigou (ISPA-INRA) for his precious help during the field campaigns,
572 especially in the installation and the maintenance of instruments.

573 **Competing interests:** The authors declare no competing of interest.

574 **References**

575 Andreae, M.O., 2013. The aerosol nucleation puzzle. Science 339, 911–912.
576 https://doi.org/10.1126/science.1233798

577 Anttila, P., Hyötyläinen, T., Heikkilä, A., Jussila, M., Finell, J., Kulmala, M., Riekkola, M.-
578 L., 2005. Determination of organic acids in aerosol particles from a coniferous forest
579 by liquid chromatography-mass spectrometry. J. Sep. Sci. 28, 337–346.
580 https://doi.org/10.1002/jssc.200401931

581 Aschmann, S., Arey, J., Atkinson, R., 2002. OH radical formation from the gas-phase
582 reactions of O3 with a series of terpenes. Atmos. Environ. 36, 4347–4355.
583 https://doi.org/10.1016/S1352-2310(02)00355-2

584 Atkinson, R., Arey, J., 2003. Gas-phase tropospheric chemistry of biogenic volatile organic
585 compounds: a review. Atmos. Environ. 37, 197–219. https://doi.org/10.1016/S1352-
586 2310(03)00391-1

587 Atkinson, R., Baulch, D.L., Cox, R.A., Crowley, J.N., Hampson, R.F., Hynes, R.G., Jenkin,
588 M.E., Rossi, M.J., Troe, J., IUPAC Subcommittee, 2006. Evaluated kinetic and
589 photochemical data for atmospheric chemistry: Volume II: gas phase reactions of
590 organic species. Atmospheric Chem. Phys. 6, 3625–4055. https://doi.org/10.5194/acp-
591 6-3625-2006

592 Aubinet, M., Grelle, A., Ibrom, A., Rannik, üLlar, Moncrieff, J., Foken, T., Kowalski, A.S.,
593 Martin, P.H., Berbigier, P., Bernhofer, C., Clement, R., Elbers, J., Granier, A.,
594 Grunwald, T., Morgenstern, K., Pilegaard, K., Rebmann, C., Snijders, W., Valentini,
595 R., Vesala, T., 2000. Estimates of the annual net carbon and water exchange of forests:
596 The EUROFLUX methodology. Adv. Ecol. Res. 30, 113–175.
597 https://doi.org/10.1016/S0065-2504(08)60018-5

598 Bäck, J., Aalto, J., Henriksson, M., Hakola, H., He, Q., Boy, M., 2012. Chemodiversity of a
599 Scots pine stand and implications for terpene air concentrations. Biogeosciences 9,
600 689–702. https://doi.org/10.5194/bg-9-689-2012

601 Baron, P.A., Willeke, K., 2001. Aerosol measurement: principles, techniques, and
602 applications. Wiley.

603 Bianchi, F., Trostl, J., Junninen, H., Frege, C., Henne, S., Hoyle, C.R., Molteni, U.,
604 Herrmann, E., Adamov, A., Bukowiecki, N., Chen, X., Duplissy, J., Gysel, M.,
605 Hutterli, M., Kangasluoma, J., Kontkanen, J., Kurten, A., Manninen, H.E., Munch, S.,
606 Perakyla, O., Petaja, T., Rondo, L., Williamson, C., Weingartner, E., Curtius, J.,
607 Worsnop, D.R., Kulmala, M., Dommen, J., Baltensperger, U., 2016. New particle
608 formation in the free troposphere: A question of chemistry and timing. Science 352,
609 1109–1112. https://doi.org/10.1126/science.aad5456

610 Bourtsoukidis, E., Williams, J., Kesselmeier, J., Jacobi, S., Bonn, B., 2014. From emissions to
611 ambient mixing ratios: online seasonal field measurements of volatile organic
612 compounds over a Norway spruce-dominated forest in central Germany. Atmospheric
613 Chem. Phys. 14, 6495–6510. https://doi.org/10.5194/acp-14-6495-2014

614 Burba, G., Anderson, D., 2010. A brief practical guide to eddy covariance flux measurements:
615 principles and workflow examples for scientific and industrial applications. Li-Cor
616 Biosciences.

617 Calogirou, A., Larsen, B.R., Kotzias, D., 1999. Gas-phase terpene oxidation products: a
618 review. Atmos. Environ. 33, 1423–1439. https://doi.org/10.1016/S1352-
619 2310(98)00277-5

Claeys, M., Iinuma, Y., Szmigielski, R., Surratt, J.D., Blockhuys, F., Van Alsenoy, C., Boge, O., Sierau, B., Gomez-Gonzalez, Y., Vermeylen, R., others, 2009. Terpenylic acid and related compounds from the oxidation of α-pinene: Implications for new particle formation and growth above forests. Environ. Sci. Technol. 43, 6976–6982.

Dal Maso, M., Kulmala, M., Riipinen, I., Wagner, R., Hussein, T., Aalto, P.P., Lehtinen, K.E.J., 2005. Formation and growth rates of ultrafine atmospheric particles: a review of observations. Boreal Environ. Res. 10, 323–336. https://doi.org/10.1016/j.jaerosci.2003.10.003

de Gouw, J., Warneke, C., 2007. Measurements of volatile organic compounds in the earth's atmosphere using proton-transfer-reaction mass spectrometry. Mass Spectrom. Rev. 26, 223–257. https://doi.org/10.1002/mas.20119

Duporté, G., Parshintsev, J., Barreira, L.M.F., Hartonen, K., Kulmala, M., Riekkola, M.-L., 2016. Nitrogen-containing low volatile compounds from pinonaldehyde-dimethylamine reaction in the atmosphere: a laboratory and field study. Environ. Sci. Technol. 50, 4693–4700. https://doi.org/10.1021/acs.est.6b00270

Ehn, M., Thornton, J.A., Kleist, E., Sipilä, M., Junninen, H., Pullinen, I., Springer, M., Rubach, F., Tillmann, R., Lee, B., Lopez-Hilfiker, F., Andres, S., Acir, I.-H., Rissanen, M., Jokinen, T., Schobesberger, S., Kangasluoma, J., Kontkanen, J., Nieminen, T., Kurtén, T., Nielsen, L.B., Jørgensen, S., Kjaergaard, H.G., Canagaratna, M., Maso, M.D., Berndt, T., Petäjä, T., Wahner, A., Kerminen, V.-M., Kulmala, M., Worsnop, D.R., Wildt, J., Mentel, T.F., 2014. A large source of low-volatility secondary organic aerosol. Nature 506, 476–479. https://doi.org/10.1038/nature13032

Elm, J., Kurtén, T., Bilde, M., Mikkelsen, K.V., 2014. Molecular interaction of pinic acid with sulfuric acid - exploring the thermodynamic landscape of cluster growth. J. Phys. Chem. A 118, 7892–7900. https://doi.org/10.1021/jp503736s

Faiola, C.L., Wen, M., VanReken, T.M., 2014. Chemical characterization of biogenic SOA generated from plant emissions under baseline and stressed conditions: inter- and intra-species variability for six coniferous species. Atmospheric Chem. Phys. Discuss. 14, 25167–25212. https://doi.org/10.5194/acpd-14-25167-2014

Faloona, I., Tan, D., Brune, W., Hurst, J., Barket Jr, D., Couch, T.L., Shepson, P., Apel, E., Riemer, D., Thornberry, T., Caroll, M.A., Sillman, S., Keeler, G.J., Sagady, J., Hooper, D., Paterson, K., 2001. Nightime observations of anomalous high levels of hydroxyl radicals above a deciduous forest canopy. J. Geophys. Res. 106, 24,315-24,333.

Feltracco, M., Barbaro, E., Contini, D., Zangrando, R., Toscano, G., Battistel, D., Barbante, C., Gambaro, A., 2018. Photo-oxidation products of α-pinene in coarse, fine and ultrafine aerosol: A new high sensitive HPLC-MS/MS method. Atmos. Environ. 180, 149–155.

Fick, J., Pommer, L., Andersson, B., Nilson, C., 2002. OH radical formation from the gas-phase reactions of O3 with a series of terpenes. Atmos. Environ. 36, 3299–3308. https://doi.org/10.1016/S1352-2310(02)00291-1

Forester, C.D., Wells, J.R., 2011. Hydroxyl radical yields from reactions of terpene mixtures with ozone: Hydroxyl radical yields from reactions of terpene mixtures with ozone. Indoor Air 21, 400–409. https://doi.org/10.1111/j.1600-0668.2011.00718.x

Gratien, A., Johnson, S.N., Ezell, M.J., Dawson, M.L., Bennett, R., Finlayson-Pitts, B.J., 2011. Surprising formation of p-Cymene in the oxidation of α-pinene in air by the atmospheric oxidants OH, O3 , and NO3. Environ. Sci. Technol. 45, 2755–2760. https://doi.org/10.1021/es103632b

Gu, L., Meyers, T., Pallardy, S.G., Hanson, P.J., Yang, B., Heuer, M., Hosman, K.P., Riggs, J.S., Sluss, D., Wullschleger, S.D., 2006. Direct and indirect effects of atmospheric conditions and soil moisture on surface energy partitioning revealed by a prolonged drought at a temperate forest site. J. Geophys. Res. 111. https://doi.org/10.1029/2006JD007161

Guenther, A., Hewitt, C.N., Erickson, D., Fall, R., Geron, C., Graedel, T., Harley, P., Klinger, L., Lerdeau, M., McKay, W.A., Pierce, T., Scholes, B., Steinbrecher, R., Tallamraju, R., Taylor, J., Zimmerman, P., 1995. A global model of natural volatile organic compound emissions. J. Geophys. Res. 100. https://doi.org/10.1029/94JD02950

Hallquist, M., Wenger, J.C., Baltensperger, U., Rudich, Y., Simpson, D., Claeys, M., Dommen, J., Donahue, N.M., Georges, C., Goldstein, A.H., Hamilton, J.F., Herrmann, H., Hoffmann, T., Iinuma, Y., Jang, M., Jenkin, M.E., Jimenez, J.L., Kiendler-Scharr, A., Maenhaut, W., McFiggans, G.B., Mentel, Th.F., Monod, A., Prevot, A.S.H., Seinfeld, J.H., Surratt, J.D., Szmigielski, R., Wildt, J., 2009. The formation, properties and impact of secondary organic aerosol: current and emerging issues. Atmospheric Chem. Phys. 9, 5155–5236. https://doi.org/10.5194/acp-9-5155-2009

Holzinger, R., Millet, D.B., Williams, B., Lee, A., Kreisberg, N., Hering, S.V., Jimenez, J., Allan, J.D., Worsnop, D.R., Goldstein, A.H., 2007. Emission, oxidation, and secondary organic aerosol formation of volatile organic compounds as observed at Chebogue Point, Nova Scotia: VOC emission and SOA formation. J. Geophys. Res. Atmospheres 112. https://doi.org/10.1029/2006JD007599

IPCC, 2013. Working group 1 conribution to the fifth assesment report - Climate change 2013- The physical science basis.

Jaoui, M., Kleindienst, T.E., Lewandowski, M., Offenberg, J.H., Edney, E.O., 2005. Identification and quantification of aerosol polar oxygenated compounds bearing carboxylic or hydroxyl groups. 2. Organic tracer compounds from monoterpenes. Environ. Sci. Technol. 39, 5661–5673. https://doi.org/10.1021/es048111b

Jokinen, T., Sipilä, M., Richters, S., Kerminen, V.-M., Paasonen, P., Stratmann, F., Worsnop, D., Kulmala, M., Ehn, M., Herrmann, H., Berndt, T., 2014. Rapid autoxidation forms highly oxidized RO2 radicals in the atmosphere. Angew. Chem. Int. Ed. 53, 14596–14600. https://doi.org/10.1002/anie.201408566

Kammer, J., Lamaud, E., Bonnefond, J.M., Garrigou, D., Flaud, P.-M., Perraudin, E., Villenave, E., 2019. Ozone production in a maritime pine forest in water-stressed conditions. Atmos. Environ. 197, 131–140. https://doi.org/10.1016/j.atmosenv.2018.10.021

Kammer, J., Perraudin, E., Flaud, P.-M., Lamaud, E., Bonnefond, J.M., Villenave, E., 2018. Observation of nighttime new particle formation over the French Landes forest. Sci. Total Environ. 621, 1084–1092. https://doi.org/10.1016/j.scitotenv.2017.10.118

Kavouras, I.G., Mihalopoulos, N., Stephanou, E.G., 1999. Formation and gas/particle partitioning of monoterpenes photo-oxidation products over forests. Nature 26, 55–58.

Kazil, J., Stier, P., Zhang, K., Quaas, J., Kinne, S., O'Donnell, D., Rast, S., Esch, M., Ferrachat, S., Lohmann, U., Feichter, J., 2010. Aerosol nucleation and its role for clouds and Earth's radiative forcing in the aerosol-climate model ECHAM5-HAM. Atmospheric Chem. Phys. 10, 10733–10752. https://doi.org/10.5194/acp-10-10733-2010

Kesselmeier, J., Staudt, M., 1999. Biogenic Volatile Organic Compounds (VOC): An Overview on Emission, Physiology and Ecology 33, 23–88.

Kim, S., Karl, T., Guenther, A., Tyndall, G., Orlando, J., Harley, P., Rasmussen, R., Apel, E., 2010. Emissions and ambient distributions of Biogenic Volatile Organic Compounds (BVOC) in a ponderosa pine ecosystem: interpretation of PTR-MS mass spectra. Atmos Chem Phys 13.

Kirkby, J., Duplissy, J., Sengupta, K., Frege, C., Gordon, H., Williamson, C., Heinritzi, M., Simon, M., Yan, C., Almeida, J., Tröstl, J., Nieminen, T., Ortega, I.K., Wagner, R., Adamov, A., Amorim, A., Bernhammer, A.-K., Bianchi, F., Breitenlechner, M., Brilke, S., Chen, X., Craven, J., Dias, A., Ehrhart, S., Flagan, R.C., Franchin, A., Fuchs, C., Guida, R., Hakala, J., Hoyle, C.R., Jokinen, T., Junninen, H., Kangasluoma, J., Kim, J., Krapf, M., Kürten, A., Laaksonen, A., Lehtipalo, K., Makhmutov, V., Mathot, S., Molteni, U., Onnela, A., Peräkylä, O., Piel, F., Petäjä, T., Praplan, A.P., Pringle, K., Rap, A., Richards, N.A.D., Riipinen, I., Rissanen, M.P., Rondo, L., Sarnela, N., Schobesberger, S., Scott, C.E., Seinfeld, J.H., Sipilä, M., Steiner, G., Stozhkov, Y., Stratmann, F., Tomé, A., Virtanen, A., Vogel, A.L., Wagner, A.C., Wagner, P.E., Weingartner, E., Wimmer, D., Winkler, P.M., Ye, P., Zhang, X., Hansel, A., Dommen, J., Donahue, N.M., Worsnop, D.R., Baltensperger, U., Kulmala, M., Carslaw, K.S., Curtius, J., 2016. Ion-induced nucleation of pure biogenic particles. Nature 533, 521–526. https://doi.org/10.1038/nature17953

Kourtchev, I., Fuller, S.J., Giorio, C., Healy, R.M., Wilson, E., O'Connor, I., Wenger, J.C., McLeod, M., Aalto, J., Ruuskanen, T.M., Maenhaut, W., Jones, R., Venables, D.S., Sodeau, J.R., Kulmala, M., Kalberer, M., 2014. Molecular composition of biogenic secondary organic aerosols using ultrahigh-resolution mass spectrometry: comparing laboratory and field studies. Atmospheric Chem. Phys. 14, 2155–2167. https://doi.org/10.5194/acp-14-2155-2014

Kristensen, K., Bilde, M., Aalto, P.P., Petäjä, T., Glasius, M., 2016. Denuder/filter sampling of organic acids and organosulfates at urban and boreal forest sites: Gas/particle distribution and possible sampling artifacts. Atmos. Environ. 130, 36–53. https://doi.org/10.1016/j.atmosenv.2015.10.046

Kristensen, K., Engrobb, K.L., King, S.M., Worton, D.R., Platt, S.M., Mortensen, R., Rosenoern, T., Surratt, J.D., Bilde, M., Goldstein, A.H., Glasius, M., 2013. Formation and occurrence of dimer esters of pinene oxidation products in atmospheric aerosols. Atmospheric Chem. Phys. 13, 3763–3776. https://doi.org/10.5194/acp-13-3763-2013

Kulmala, M., 2003. How particles nucleate and grow. Science 302, 1000–1001. https://doi.org/10.1126/science.1090848

Kulmala, M., Kontkanen, J., Junninen, H., Lehtipalo, K., Manninen, H.E., Nieminen, T., Petaja, T., Sipila, M., Schobesberger, S., Rantala, P., Franchin, A., Jokinen, T., Jarvinen, E., Aijala, M., Kangasluoma, J., Hakala, J., Aalto, P.P., Paasonen, P., Mikkila, J., Vanhanen, J., Aalto, J., Hakola, H., Makkonen, U., Ruuskanen, T., Mauldin, R.L., Duplissy, J., Vehkamaki, H., Back, J., Kortelainen, A., Riipinen, I., Kurten, T., Johnston, M.V., Smith, J.N., Ehn, M., Mentel, T.F., Lehtinen, K.E.J.,

Laaksonen, A., Kerminen, V.-M., Worsnop, D.R., 2013. Direct Observations of Atmospheric Aerosol Nucleation. Science 339, 943–946. https://doi.org/10.1126/science.1227385

Kulmala, M., Vehkamäki, H., Petäjä, T., Dal Maso, M., Lauri, A., Kerminen, V.-M., Birmili, W., McMurry, P.H., 2004. Formation and growth rates of ultrafine atmospheric particles: a review of observations. J. Aerosol Sci. 35, 143–176. https://doi.org/10.1016/j.jaerosci.2003.10.003

Laothawornkitkul, J., Taylor, J.E., Paul, N.D., Hewitt, C.N., 2009. Biogenic volatile organic compounds in the Earth system. New Phytol. 183, 27–51. https://doi.org/10.1111/j.1469-8137.2009.02859.x

Lathiere, J., Hauglustaine, D.A., Friend, A.D., Noblet-Ducoudre, N.D., Viovy, N., Folberth, G.A., 2006. Impact of climate variability and land use changes on global biogenic volatile organic compound emissions. Atmos Chem Phys 18.

Lee, A., Goldstein, A.H., Keywood, M.D., Gao, S., Varutbangkul, V., Bahreini, R., Ng, N.L., Flagan, R.C., Seinfeld, J.H., 2006. Gas-phase products and secondary aerosol yields from the ozonolysis of ten different terpenes. J. Geophys. Res. 111. https://doi.org/10.1029/2005JD006437

Loreto, F., Förster, A., Dürr, M., Csiky, O., Seuffert, G., 1998. On the monoterpene emission under heat stress and on the increased thermotolerance of leaves of Quercus ilex L. fumigated with selected monoterpenes. Plant Cell Environ. 21, 101–107.

Merikanto, J., Spracklen, D.V., Mann, G.W., Pickering, S.J., Carslaw, K.S., 2009. Impact of nucleation on global CCN. Atmospheric Chem. Phys. 9, 8601–8616. https://doi.org/10.5194/acp-9-8601-2009

Mochizuki, T., Tani, A., Takahashi, Y., Saigusa, N., Ueyama, M., 2014. Long-term measurement of terpenoid flux above a Larix kaempferi forest using a relaxed eddy accumulation method. Atmos. Environ. 83, 53–61. https://doi.org/10.1016/j.atmosenv.2013.10.054

Moreaux, V., Lamaud, E., Bosc, A., Bonnefond, J.-M., Medlyn, B.E., Loustau, D., 2011. Paired comparison of water, energy and carbon exchanges over two young maritime pine stands (Pinus pinaster Ait.): effects of thinning and weeding in the early stage of tree growth. Tree Physiol. 31, 903–921. https://doi.org/10.1093/treephys/tpr048

Nallathamby, P.D., Hopke, P.K., Rossner, A., Dhaniyala, S., Marzocca, P., Petaja, T., Barthelmie, R.J., Pryor, S.C., 2014. Particle nucleation in a forested environment. Atmospheric Pollut. Res. 5, 805–810. https://doi.org/10.5094/APR.2014.090

Neitola, K., Brus, D., Makkonen, U., Sipilä, M., Mauldin III, R.L., Sarnela, N., Jokinen, T., Lihavainen, H., Kulmala, M., 2015. Total sulfate vs. sulfuric acid monomer concenterations in nucleation studies. Atmospheric Chem. Phys. 15, 3429–3443. https://doi.org/10.5194/acp-15-3429-2015

Nozière, B., González, N.J.D., Borg-Karlson, A.-K., Pei, Y., Redeby, J.P., Krejci, R., Dommen, J., Prevot, A.S.H., Anthonsen, T., 2011. Atmospheric chemistry in stereo: A new look at secondary organic aerosols from isoprene. Geophys. Res. Lett. 38, n/a-n/a. https://doi.org/10.1029/2011GL047323

Nozière, B., Kalberer, M., Claeys, M., Allan, J., D'Anna, B., Decesari, S., Finessi, E., Glasius, M., Grgić, I., Hamilton, J.F., Hoffmann, T., Iinuma, Y., Jaoui, M., Kahnt, A., Kampf, C.J., Kourtchev, I., Maenhaut, W., Marsden, N., Saarikoski, S., Schnelle-

Kreis, J., Surratt, J.D., Szidat, S., Szmigielski, R., Wisthaler, A., 2015. The Molecular Identification of Organic Compounds in the Atmosphere: State of the Art and Challenges. Chem. Rev. 115, 3919–3983. https://doi.org/10.1021/cr5003485

Pang, X., 2015. Biogenic volatile organic compound analyses by PTR-TOF-MS: Calibration, humidity effect and reduced electric field dependency. J. Environ. Sci. 32, 196–206. https://doi.org/10.1016/j.jes.2015.01.013

Park, J.-H., Fares, S., Weber, R., Goldstein, A.H., 2014. Biogenic volatile organic compound emissions during BEARPEX 2009 measured by eddy covariance and flux–gradient similarity methods. Atmospheric Chem. Phys. 14, 231–244. https://doi.org/10.5194/acp-14-231-2014

Park, J.-H., Goldstein, A.H., Timkovsky, J., Fares, S., Weber, R., Karlik, J., Holzinger, R., 2013. Eddy covariance emission and deposition flux measurements using proton transfer reaction - time of flight - mass spectrometry (PTR-TOF-MS): comparison with PTR-MS measured vertical gradients and fluxes. Atmospheric Chem. Phys. 13, 1439–1456. https://doi.org/10.5194/acp-13-1439-2013

Peñuelas, J., Staudt, M., 2010. BVOCs and global change. Trends Plant Sci. 15, 133–144. https://doi.org/10.1016/j.tplants.2009.12.005

Pope III, C.A., Dockery, D.W., 2006. Health effects of fine particulate air pollution: lines that connect. J. Air Waste Manag. Assoc. 56, 709–742.

Praplan, A.P., Schobesberger, S., Bianchi, F., Rissanen, M.P., Ehn, M., Jokinen, T., Junninen, H., Adamov, A., Amorim, A., Dommen, J., Duplissy, J., Hakala, J., Hansel, A., Heinritzi, M., Kangasluoma, J., Kirkby, J., Krapf, M., Kürten, A., Lehtipalo, K., Riccobono, F., Rondo, L., Sarnela, N., Simon, M., Tomé, A., Tröstl, J., Winkler, P.M., Williamson, C., Ye, P., Curtius, J., Baltensperger, U., Donahue, N.M., Kulmala, M., Worsnop, D.R., 2015. Elemental composition and clustering behaviour of α-pinene oxidation products for different oxidation conditions. Atmospheric Chem. Phys. 15, 4145–4159. https://doi.org/10.5194/acp-15-4145-2015

Rantala, P., Taipale, R., Aalto, J., Kajos, M.K., Patokoski, J., Ruuskanen, T.M., Rinne, J., 2014. Continuous flux measurements of VOCs using PTR-MS—reliability and feasibility of disjunct-eddy-covariance, surface-layer-gradient, and surface-layer-profile methods. Boreal Environ. Res. 19, 87–107.

Riba, M.-L., Tathy, J.P., Tsiropoulos, N., Monsarrat, B., Torres, L., 1987. Diurnal variation in the concentration of α- and β- pinene in the Landes forest (France). Atmos. Environ. 21, 191–193. https://doi.org/10.1034/j.1600-0889.2001.530411.x

Riccobono, F., Schobesberger, S., Scott, C.E., Dommen, J., Ortega, I.K., Rondo, L., Almeida, J., Amorim, A., Bianchi, F., Breitenlechner, M., David, A., Downard, A., Dunne, E.M., Duplissy, J., Ehrhart, S., Flagan, R.C., Franchin, A., Hansel, A., Junninen, H., Kajos, M., Keskinen, H., Kupc, A., Kurten, A., Kvashin, A.N., Laaksonen, A., Lehtipalo, K., Makhmutov, V., Mathot, S., Nieminen, T., Onnela, A., Petaja, T., Praplan, A.P., Santos, F.D., Schallhart, S., Seinfeld, J.H., Sipila, M., Spracklen, D.V., Stozhkov, Y., Stratmann, F., Tome, A., Tsagkogeorgas, G., Vaattovaara, P., Viisanen, Y., Vrtala, A., Wagner, P.E., Weingartner, E., Wex, H., Wimmer, D., Carslaw, K.S., Curtius, J., Donahue, N.M., Kirkby, J., Kulmala, M., Worsnop, D.R., Baltensperger, U., 2014. Oxidation products of biogenic emissions contribute to nucleation of atmospheric particles. Science 344, 717–721. https://doi.org/10.1126/science.1243527

Rickard, A.R., Johnson, D., McGill, C.D., Marston, G., 1999. OH Yields in the Gas-Phase Reactions of Ozone with Alkenes. J. Phys. Chem. A 103, 7656–7664. https://doi.org/10.1021/jp9916992

Rose, C., Zha, Q., Dada, L., Yan, C., Lehtipalo, K., Junninen, H., Mazon, S.B., Jokinen, T., Sarnela, N., Sipilä, M., Petäjä, T., Kerminen, V.-M., Bianchi, F., Kulmala, M., 2018. Observations of biogenic ion-induced cluster formation in the atmosphere. Sci. Adv. 4, eaar5218. https://doi.org/10.1126/sciadv.aar5218

Ruuskanen, T.M., Müller, M., Schnitzhofer, R., Karl, T., Graus, M., Bamberger, I., Hörtnagl, L., Brilli, F., Wohlfahrt, G., Hansel, A., 2011. Eddy covariance VOC emission and deposition fluxes above grassland using PTR-TOF. Atmospheric Chem. Phys. 11, 611–625. https://doi.org/10.5194/acp-11-611-2011

Seinfeld, J.H., Pandis, S.N., 2006. Atmospheric Chemistry and Physics: From Air Pollution to Climate Change, 2nd Edition. ed. Wiley-Blackwell, Hoboken, N.J.

Simon, V., Clement, B., Riba, M.-L., Torres, L., 1994. The Landes experiment: Monoterpenes emitted from the maritime pine. J. Geophys. Res. 99, 16501–16510. https://doi.org/10.1029/94JD00785

Sindelarova, K., Granier, C., Bouarar, I., Guenther, A., Tilmes, S., Stavrakou, T., Müller, J.-F., Kuhn, U., Stefani, P., Knorr, W., 2014. Global dataset of biogenic VOC emissions calculated by the MEGAN model over the last 30 years. Atmospheric Chem. Phys. Discuss. 14, 10725–10788. https://doi.org/10.5194/acpd-14-10725-2014

Sipilä, M., Jokinen, T., Berndt, T., Richters, S., Makkonen, R., Donahue, N.M., Mauldin III, R.L., Kurtén, T., Paasonen, P., Sarnela, N., Ehn, M., Junninen, H., Rissanen, M.P., Thornton, J., Stratmann, F., Herrmann, H., Worsnop, D.R., Kulmala, M., Kerminen, V.-M., Petäjä, T., 2014. Reactivity of stabilized Criegee intermediates (sCIs) from isoprene and monoterpene ozonolysis toward SO2; and organic acids. Atmospheric Chem. Phys. 14, 12143–12153. https://doi.org/10.5194/acp-14-12143-2014

Staudt, M., Lhoutellier, L., 2011. Monoterpene and sesquiterpene emissions from <i>Quercus coccifera</i> exhibit interacting responses to light and temperature. Biogeosciences 8, 2757–2771. https://doi.org/10.5194/bg-8-2757-2011

Stein, A.F., Draxler, R.R., Rolph, G.D., Stunder, B.J.B., Cohen, M.D., Ngan, F., 2015. NOAA's HYSPLIT atmospheric transport and dispersion modeling system. Bull. Am. Meteorol. Soc. 96, 2059–2077. https://doi.org/10.1175/BAMS-D-14-00110.1

Tani, A., Hayward, S., Hewitt, C.N., 2003. Measurement of monoterpenes and related compounds by proton transfer reaction-mass spectrometry (PTR-MS). Int. J. Mass Spectrom. 223, 561–578.

Tröstl, J., Chuang, W.K., Gordon, H., Heinritzi, M., Yan, C., Molteni, U., Ahlm, L., Frege, C., Bianchi, F., Wagner, R., Simon, M., Lehtipalo, K., Williamson, C., Craven, J.S., Duplissy, J., Adamov, A., Almeida, J., Bernhammer, A.-K., Breitenlechner, M., Brilke, S., Dias, A., Ehrhart, S., Flagan, R.C., Franchin, A., Fuchs, C., Guida, R., Gysel, M., Hansel, A., Hoyle, C.R., Jokinen, T., Junninen, H., Kangasluoma, J., Keskinen, H., Kim, J., Krapf, M., Kürten, A., Laaksonen, A., Lawler, M., Leiminger, M., Mathot, S., Möhler, O., Nieminen, T., Onnela, A., Petäjä, T., Piel, F.M., Miettinen, P., Rissanen, M.P., Rondo, L., Sarnela, N., Schobesberger, S., Sengupta, K., Sipilä, M., Smith, J.N., Steiner, G., Tomè, A., Virtanen, A., Wagner, A.C., Weingartner, E., Wimmer, D., Winkler, P.M., Ye, P., Carslaw, K.S., Curtius, J., Dommen, J., Kirkby, J., Kulmala, M., Riipinen, I., Worsnop, D.R., Donahue, N.M.,

Baltensperger, U., 2016. The role of low-volatility organic compounds in initial particle growth in the atmosphere. Nature 533, 527–531. https://doi.org/10.1038/nature18271

United Nations food and agricultural organization, 2015. Evaluation des ressources forestières mondiales (No. 1). Rome.

Vestenius, M., Hellén, H., Levula, J., Kuronen, P., Helminen, K.J., Nieminen, T., Kulmala, M., Hakola, H., 2014. Acidic reaction products of mono- and sesquiterpenes in atmospheric fine particles in a boreal forest. Atmospheric Chem. Phys. Discuss. 14, 2857–2881. https://doi.org/10.5194/acpd-14-2857-2014

Yasmeen, F., Szmigielski, R., Vermeylen, R., Gomez-Gonzalez, Y., Surratt, J.D., Chan, A.W.H., Seinfeld, J.H., Maenhaut, W., Claeys, M., 2011. Mass spectrometric characterization of isomeric terpenoic acids from the oxidation of α-pinene, β-pinene, d-limonene, and delta-3-carene in fine forest aerosol. J. Mass Spectrom. 46, 425–442. https://doi.org/10.1002/jms.1911